HHS Public Access

Author manuscript

*Toxicol Lett*. Author manuscript; available in PMC 2021 August 01.

Published in final edited form as:

*Toxicol Lett*. 2020 August 01; 328: 52–60. doi:10.1016/j.toxlet.2020.04.010.

# *In vivo* and *In vitro* Inflammatory Responses to Fine Particulate Matter ($PM_{2.5}$) from China and California

**Wanjun Yuan**[a,b,1], **Ciara C. Fulgar**[b,1], **Xiaolin Sun**[b,c,1], **Christoph F. A. Vogel**[b,d], **Ching-Wen Wu**[b], **Qi Zhang**[d], **Keith J. Bein**[b], **Dominique E. Young**[d], **Wei Li**[c], **Haiying Wei**[a], **Kent E. Pinkerton**[b]

[a]College of Environmental and Resource Sciences, Shanxi University, Taiyuan, China

[b]Center for Health and the Environment, University of California, Davis, USA

[c]Biomedical Engineering Institute, School of Control Science and Engineering, Shandong University, Jinan, China

[d]Department of Environmental Toxicology, University of California, Davis, USA

## Abstract

Ambient $PM_{2.5}$ was collected during the winter season from Taiyuan, Shanxi, China; Jinan, Shandong, China; and Sacramento, California, USA, and used to create $PM_{SX}$, $PM_{SD}$, and $PM_{CA}$ extracts, respectively. Time-lag experiments were performed to explore the *in vivo* and *in vitro* toxicity of the PM extracts. *In vivo* inflammatory lung responses were assessed in BALB/C mice using a single oropharyngeal aspiration (OPA) of PM extract or vehicle (CTRL) on Day 0. Necropsies were performed on Days 1, 2, and 4 post-OPA, and pulmonary effects were determined using bronchoalveolar lavage (BAL) and histopathology. On Day 1, BAL neutrophils were significantly elevated in all PM- versus CTRL-exposed mice, with $PM_{CA}$ producing the strongest response. However, histopathological scoring showed greater alveolar and perivascular effects in $PM_{SX}$-exposed mice compared to all three other groups. By Day 4, BAL neutrophilia and tissue inflammation were resolved, similar across all groups. *In vitro* effects were examined in human HepG2 hepatocytes, and U937 cells following 6, 24, or 48 hours of exposure to PM extract or DMSO (control). Luciferase reporter and quantitative polymerase chain reaction assays were used to determine *in vitro* effects on aryl hydrocarbon receptor (AhR) activation and gene transcription, respectively. Though all three PM extracts activated AhR, $PM_{SX}$ produced the greatest increases in AhR activation, and mRNA levels of cyclooxygenase-2, cytochrome P450, interleukin (IL)-8, and

Corresponding Authors: 1. Haiying Wei, College of Environmental and Resource Sciences, Shanxi University, Taiyuan, China weihaiying@sxu.edu.cn, 2. Wei Li, Shandong University, Biomedical Engineering Institute, School of Control Science and Engineering, Jinan, China cindy@sdu.edu.cn, 3. Kent E. Pinkerton, SENIOR AUTHOR: Center for Health and the Environment, University of California, Davis, USA kepinkerton@ucdavis.edu.

[1]These authors contributed equally to the research.

Declaration of interests

The authors declare that they have no known competing financial interests or personal relationships that could have appeared to influence the work reported in this paper.

*IL-1β*. These effects were assumed to result from a greater abundance of polycyclic aromatic hydrocarbons (PAHs) in $PM_{SX}$ compared to $PM_{SD}$ and $PM_{CA}$.

## Graphical abstract

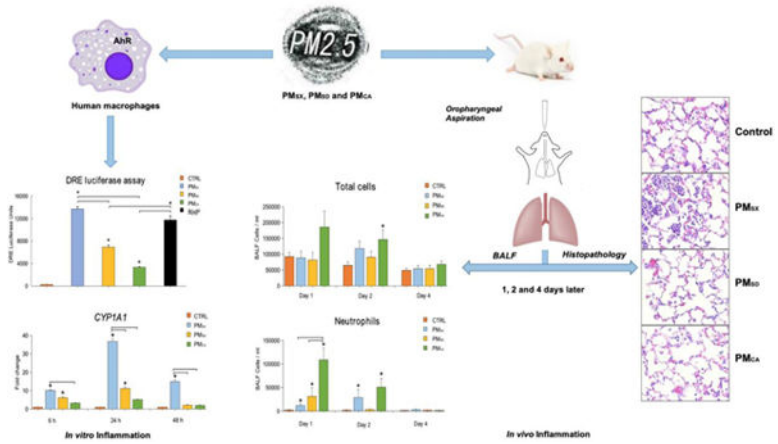


### Keywords

$PM_{2.5}$; air pollution; time-lag study; human macrophages; aryl hydrocarbon receptor

## 1. INTRODUCTION

The lung is one of the major targets for particulate matter (PM) deposition. Ambient fine particulate matter ($PM_{2.5}$; diameter ≤$_{2.5}$ μm), a prevalent component of air pollution, consists of a heterogeneous mixture of airborne solid and liquid particles (Kelly and Fussell, 2012). $PM_{2.5}$ inhaled through the nose and mouth can penetrate deep into the lungs, deposit in the airways and alveoli, and pass into systemic circulation to elicit responses in pulmonary and extrapulmonary tissues (Craig et al., 2008; Gunasekar and Stanek, 2011; Smith et al., 2003). According to the World Health Organization (WHO, 2018), air pollution in cities and rural areas caused an estimated 4.2 million premature deaths worldwide in 2016. This mortality was likely due to $PM_{2.5}$ exposure, which has been associated with cardiovascular and respiratory diseases including myocardial infarction, atherosclerosis, acute bronchitis and upper airway infection (Pinkerton et al., 2019). Inhalation of PM can also exacerbate persistent airway diseases such as chronic obstructive pulmonary disease and asthma (WHO, 2018). Extensive research has shown PM can vary by time and location (Krewski et al., 2005), while toxicity can be highly dependent on physicochemical composition and exposure conditions (Di Filippo et al., 2007; Laurent et al., 2016).

In the present study, $PM_{2.5}$ was collected from Taiyuan and Jinan, capital cities of the Chinese provinces, Shanxi and Shandong, respectively, and Sacramento, the capital of California. In Shanxi, 34 million tons of coal was produced in 2013, accounting for 2.5% of the total annual coal production in China (Tang et al., 2014). In Shandong, from 2011 to 2015, numerous chemical factories may have contributed to 209,321 deaths in people suffering respiratory and cardiovascular diseases associated with increased provincial PM

concentrations (Zhang et al., 2017). In the intermountain region of California's Central Valley, including Sacramento and seventeen other counties, the terrain is highly susceptible to meteorological inversions, air stagnation, and air pollution accumulation. Such conditions create an environmental airshed (a geographical area where the air is typically confined or channeled to become uniformly polluted and stagnant) that places residents at increased risk for exposure to particles. The Central Valley encompasses a rich farming region, as well as extensive urban development (Holmes et al., 2015; Pinkerton et al., 2000). Taiyuan, Jinan, and Sacramento, all heavily urbanized cities, have long, dry winter seasons and long-standing histories of unhealthy $PM_{2.5}$ pollution. The goal of the current study was to extend previously published work (Sun et al., 2017; Zhang et al., 2018) as a means to better understand how PM from different sources can influence *in vivo* and *in vitro* toxicity over time.

Macrophages are critical cells of the primary innate immune response in the lungs. Pulmonary macrophages form a heterogeneous population of immune cells that fulfill a variety of specialized functions, including maintenance of pulmonary homeostasis, cellular debris removal, immune surveillance, microbial clearance, infection response, and inflammation resolution (Byrne et al., 2015; Suwa et al., 2002). Suwa *et al.* (2002) found exposure of rabbits to $PM_{10}$ (diameter ≥ 10 μm) caused progression of atherosclerotic lesions, as well as numerous particle-laden macrophages, suggesting an association between PM exposure and a robust inflammatory response. Macrophage recruitment to the conducting airways, alveoli, and blood vessels may be considered an indication of histopathologic acute lung inflammation (Aggarwal et al., 2014).

PM can contain a wide variety of chemicals, including polycyclic aromatic hydrocarbons (PAHs) known to activate the aryl hydrocarbon receptor (AhR). The AhR is a cytoplasmic ligand-activated transcription factor that mediates many of the toxic responses to environmental chemicals such as benzo[a]pyrene (B[a]P); 2,3,7,8-tetrachlorodibenzo-p-dioxin (TCDD); or dioxin-like polychlorinated biphenyls (PCBs). Following ligand binding, the activated AhR associates with the AhR nuclear translocator (ARNT) and translocates to the nucleus. The AhR-ARNT complex binds to its specific deoxyribonucleic acid (DNA) recognition site, the dioxin responsive element (DRE), and induces the transcription of an array of target genes such as that for cytochrome P450 (Okey, 2007; Vogel et al., 2019). Several *in vitro* studies (Mathiesen et al., 2004; Vogel et al., 2007; Vogel et al., 2019) suggest PM may promote pathological processes of inflammation by inducing the expression of genes for inflammatory pathways [e.g. cyclooxygenase-2 (*COX-2*), interleukin (*IL*)-*8*, *IL-1β,* or tumor necrosis factor-alpha (*TNF-α*) genes], and AhR signaling (e.g. *COX-2* and *IL-8* genes). Vogel *et al.* (2005) showed organic extracts from urban dust or diesel exhaust induced expression of *IL-8*, *COX-2*, and *CYP1A1*, all genes considered to be involved in PM-mediated inflammatory responses in macrophages.

Since mechanisms driving PM-mediated inflammation and macrophage activation require further clarification, an *in vivo* BALB/C mouse model, and an *in vitro* human U937 macrophage model were implemented in the present study. The primary goal was to compare the initiation and duration of cellular and histological changes in the lungs due to a single acute exposure to one of three different extracts of PM collected from urban regions

known for high wintertime PM air pollution (Taiyuan, Shanxi; Jinan, Shandong; and Sacramento, California). The secondary goal was to elucidate the molecular factors and pathways that drive macrophage responses *in vitro*. To support this research, the three PM samples were extracted, analyzed, and compared to determine whether and how differences in chemical composition influence toxicity *in vivo* and/or *in vitro*. The tested hypothesis was that PM extracts from distinct sources and geographic regions elicit different inflammatory responses over time in the lungs, as well as unique gene expression in macrophages due to varying chemical composition.

## 2. MATERIALS AND METHODS

### 2.1. $PM_{2.5}$ Collection and Extraction

Ambient $PM_{2.5}$ was collected during the winter season from the cities of Taiyuan, Shanxi; Jinan, Shandong; and Sacramento, California for chemical and toxicological characterization. PM collection and extraction methods used in the present study have been described previously (Sun et al., 2017; Zhang et al., 2018), and are included herein for reader convenience.

The sampling site in downtown Taiyuan was located on the rooftop of a five-story building in the College of Environmental and Resource Sciences on the Shanxi University campus (37°47′N, 112°34′E). This campus is surrounded by a mixture of residential, commercial, and industrial buildings. Prior to sampling, 90 mm diameter Quartz microfiber filters (Whatman, WHA1851090) were preheated at 450°C for 24 hours to eliminate any potential endotoxin contamination, and pre-weighed to enable future gravimetric assessments. PM samples were collected onto the filters for one day using a high-volume particle collector (Thermo Anderson, HVAIR100) with a size-selective head and a flow rate of 40 cubic foot per minute (cfm). Following the sampling, the filters were post-weighed to calculate the collected PM mass (post weight – pre weight = PM mass), cut into filter segments for placement in a 250 mL conical flask with 30 mL Milli-Q water, and sonicated for 30 minutes (3 cycles of 10 minutes each) to produce a PM extract. The extract was filtered through six layers of sterile gauze, lyophilized to powder, and stored at −80°C.

The sampling site in downtown Jinan was located on the rooftop of a three-story building at the Wang She Ren Primary School (36°40’N, −117°09’E). Filters were pre-heated and pre-weighed, and $PM_{2.5}$ was collected in the same manner used in Taiyuan.

In downtown Sacramento, the sampling site was located on the rooftop of a two-story building at the northeast corner of T and 13th streets (38°34′N, 121°29′W); surrounded by a mixture of residential, commercial, and industrial buildings; and stationed within a quarter-mile of a major freeway interchange. $PM_{2.5}$ was collected for seven days with a high-volume sampler system (Tisch Environmental Inc., TE-6070V-2.5-HVS) equipped with a $PM_{2.5}$ size-selective head (Tisch Environmental Inc., TE-6001), operated at a flow rate of 40 cfm and loaded with pre-cleaned Teflon-coated borosilicate glass microfiber filters (Pall Corporation, TX40H120WW). Pre-sampling filter cleaning involved successive sonication in Milli-Q water, dichloromethane and hexane. Field blanks were included. The extraction procedure using a blank filter was applied and compared to each of the three PM extract

samples. These field blanks were used to confirm no extractable compounds from these filters produced a noticeable effect beyond what was noted with Milli-Q water.

Sample filters from Jinan and Sacramento were post-weighed to calculate the PM mass, placed in Milli-Q water, and sonicated for 1 hour. The sonication extracts were filtered using a 0.2 μm pore size syringe filter, and the collected solution (approximately 100 mL) was lyophilized and stored at −80°C. Detailed extraction methods have been described by Bein and Wexler (2015).

Lyophilized extracts from Taiyuan, Jinan, and Sacramento were weighed, and resuspended for a final time in either Milli-Q water to create 1 mg/mL stock extracts for chemical analysis and *in vivo* experiments, or dimethyl sulfoxide (DMSO; 0.1%) at a final concentration of 10 mg/mL for use with *in vitro* work. Both the 1 mg/mL stock and 10 mg/mL extracts made from Taiyuan, Jinan, and Sacramento PM are referred to hereafter as $PM_{SX}$, $PM_{SD}$, and $PM_{CA}$.

## 2.2. Chemical Characterization

All chemical analyses were performed in the Department of Environmental Toxicology at the University of California, Davis. Frozen 1 mg/mL $PM_{SX}$, $PM_{SD,}$ and $PM_{CA}$ stock extracts were thawed to 4°C and sonicated for 20 minutes to ensure complete, homogeneous dispersion prior to analysis by high-resolution time-of-flight mass spectrometry (HR-AMS) and inductively-coupled plasma mass spectrometry (ICP-MS).

**Measurement of Chemical Composition in PM Extracts via HR-AMS—**Stock 1 mg/mL $PM_{SX}$, $PM_{SD}$, and $PM_{CA}$ extracts were diluted by a factor of 10 to 0.1 mg/mL, and a 1 mL aliquot of each diluted extract was measured for nitrate ($NO_3^-$), sulfate ($SO_4^{2-}$), chloride ($Cl^-$), ammonium ($NH_4^+$), and organic species via HR-AMS. This technique has been used extensively to quantitatively characterize the bulk composition of ambient aerosols (Canagaratna et al., 2007). Sample aliquots in the present study were atomized using a constant output aerosol generator with an inert argon carrier gas. The generated aerosol passed through a silica gel diffusion tube before being sampled by HR-AMS. The elemental composition of the organic aerosols in each of the extracts was determined by the method of Aiken et al. (2008) to determine the average degree of oxidation of organic matter in particles. Analytical chemical characterization and data evaluation methods have been described in greater detail elsewhere (Sun et al., 2011; Zhang et al., 2018).

**Measurement of Metals in PM Extracts via ICP-MS—**$PM_{SX}$, $PM_{SD}$, and $PM_{CA}$ extracts were analyzed using an Agilent 7500ce ICP-MS for a wide range of metals, including potassium (K), calcium (Ca), Zinc (Zn), copper (Cu), magnesium (Mg), iron (Fe), lead (Pb), and nickel (Ni). Prior to analysis, 0.06 mL of concentrated nitric acid (15.968 M, Fischer Scientific) was added to each of the stock extracts, followed by the addition of Milli-Q water to create a final volume of 2 mL. The PM concentration used for ICP-MS analysis was 1 mg/mL for $PM_{SX}$, 1.8 mg/mL for $PM_{SD}$, and 1.3 mg/mL for $PM_{CA}$. These samples were nebulized to form aerosolized particles integrated by an argon carrier gas to high temperature argon plasma. Calibration samples with known concentrations were also analyzed.

### 2.3. In vivo Experiments with BALB/C Mice

**Animals and Treatment—**All procedures with animals were approved by the UC Davis Institutional Animal Care and Use Committee in accordance with the US Animal Welfare Act. A total of 72 male, 8-week old BALB/C mice were used (ENvigo, Hayward, CA). Mice were housed four per cage, on sterile laboratory bedding using a 12-hour light/dark cycle and access *ad libitum* to water and food. Prior to the start of the experiment, mice were acclimated for one week and assigned by random number generation, to one of four groups (n = 18/group). Upon initiation of the experimental period (Day 0), isoflurane gas was diluted with oxygen (3:1 ratio) and used to attain a Stage-2 level of anesthesia (retained sniff reflex) in the mice for exposure to a single 50 μL oropharyngeal aspirate of Milli-Q water vehicle sham control (CTRL) or stock 1 mg/mL extract ($PM_{SX}$, $PM_{SD}$, or $PM_{CA}$). At 1, 2, or 4 days post-oropharyngeal aspiration (OPA), mice were weighed and euthanized using a 0.2 mL intraperitoneal injection of Beuthanasia-D pentobarbital solution (65 mg/kg body weight; Nembutal, Cardinal Health, Sacramento, CA). Necropsies were performed on 24 mice/timepoint (n = 6/group), for collection and analysis of biological samples.

**Collection and Analysis of Bronchoalveolar Lavage Fluid (BALF)—**Following intratracheal cannulation and clamping of the left mainstem bronchus, the right lung lobes of each mouse was lavaged with two aliquots (0.6 mL/aliquot) of Dulbecco's Phosphate Buffered Saline (PBS; Sigma Aldrich, St Louis, MO). BALF from each mouse was centrifuged at 4°C and 2000 × g for 15 minutes to pellet the cells. The pelleted cells were resuspended in 0.5 mL PBS to determine total cell numbers and viability via Trypan Blue exclusion assay (Sigma Aldrich, St Louis, Missouri). Cytospin slides were prepared and stained with DippKwik Differential Stain kit (American MasterTech, Lodi, CA) for cell differential analysis in which 500 cells/slide were counted using a light microscope.

**Lung tissue Collection—**The left mainstem bronchus was unclamped and the left lung was inflation-fixed with 4% paraformaldehyde at 30 cm of pressure for one hour, stored in 4% paraformaldehyde for 48 hours, and transferred into 70% ethanol for embedment, sectioning, and histopathological analysis. The right lung lobes for each mouse were placed in two cryovials—one vial for the cranial and middle lobes, and the second for the caudal and accessory lobes—and stored at −80°C until further use.

**Lung tissue processing and embedment—**Four transverse slices (levels) of the inflation-fixed left lung were cut to uniformly sample the lung. These tissue slices were dehydrated through a graded series of ethanol (70, 80, 95, 100%) and toluene (50, 100%), then embedded in paraffin (Paraplast-20). Each tissue slice was sectioned at a thickness of 5 μm, placed on glass slides, stained with Harris hematoxylin and eosin (H&E; American MasterTech, Lodi, CA), and cover slipped.

**Semi-Quantitative Histopathological Assessment of Lung Tissues—**Stained lung tissue sections from each of the four different levels of the left lung were examined for the presence of cellular infiltrates; epithelial abnormalities; and alveolar, bronchiolar, and perivascular inflammation. An ordinal, semi-quantitative scoring rubric was used to rank the degree of inflammation as shown in Supplemental Table 1 (Silva et al., 2014; Silva et al.,

2013). Briefly, a blind, qualitative assessment was initially performed to evaluate the range of inflammatory responses for the four levels of the lung. The scoring rubric was then used to minimize observer subjectivity. Categorical descriptions were used to determine the degree and extent of inflammation (e.g. focal versus diffuse). Scoring for the extent of inflammation was implemented as follows: no changes (0), less than one-third of the slide (1), up to one-half of the slide (2), more than one-half of the slide (3). Pictorial guidelines of severity with scores from 0 to 3 were defined as none (0), minimal (1), moderate (2), and marked (3) inflammation, respectively. For final histological assessments, the extent and severity scores were multiplied to achieve an overall histopathological score for each animal.

### 2.4. *In vitro* Experiments in Human HepG2 (Liver Cancer) and U937 (Promonocyte, Histiocytic Lymphoma) Cells

**Dioxin-Responsive Element (DRE) Luciferase Reporter Assay—**The AhR is expressed in lung cells and has been shown to be activated by certain PAHs (Chan et al., 2014; Hawk et al., 2002). To test whether China and California PM may activate AhR, HepG2 cells (ATCC HB-8065, Manassas, VA), which are considered to have a high transfection efficiency useful in the detection of AhR activation by various ligands, were first seeded in DMEM medium (Gibco Life Technologies, Grand Island, NY) with 10% fetal bovine serum (FBS) at a density of $1.2 \times 10^4$ /well onto 24-well plate. HepG2 cells were then stable transfected with PTX.DIR containing a DRE luciferase reporter construct as described (Berghard et al., 1993). PTX.DIR consists of a xenobiotic response element sequences extending from nucleotides −1026 to −999 relative to the transcription start site of the human *CYP1A1* gene and inserted in a vector containing the herpes simplex virus thymidine kinase promoter and the luciferase reporter gene. Transfected cells were treated with (DMSO; 0.1%); 10 μg/mL $PM_{SX}$, $PM_{SD}$, or $PM_{CA}$ extract samples; or a B[a]P standard reference material (positive control) and incubated at 37°C for 4 hours. Luciferase activity was measured with the luciferase reporter assay system (Promega Corp., Madison, WI) using a luminometer (Berthold Lumat LB 9501/16, Pittsburg, PA). Experiments were performed in triplicate, and data were expressed as relative light units.

**U937 Cell Culture Assays—**Human U937 monocytic cells were obtained from the American Tissue Culture Collection (Manassas, VA) and maintained in RPMI 1640 growth medium containing 10% FBS (Gibco Life Technologies, Grand Island, NY), 100 U penicillin, and 100 μg/mL streptomycin supplemented with 4.5 g/L glucose, 1 mM sodium pyruvate, and 10 mM HEPES. Cell cultures were maintained at a cell concentration between $2 \times 10^5$ and $2 \times 10^6$ cells/mL. To induce their differentiation into macrophages, U937 cells were treated with TPA (2-O-tetradecanoylphorbol-13-acetate; 5 μg/mL) and allowed to adhere for 48 hours in a 5% $CO_2$ tissue-culture incubator at 37°C (Vogel et al., 2012). Afterward, cells were treated with 10 μg/mL $PM_{SX}$, $PM_{SD}$, or $PM_{CA}$ extract samples; or B[a]P, DMSO at 0.1% in culture medium was used as vehicle control, and incubated at 37°C for 6, 24, or 48 hours prior to use in molecular assays.

**Ribonucleic Acid (RNA) Isolation and Quantitative Real-Time reverse transcription-Polymerase Chain Reaction (qRT-PCR)—**RNA was isolated from the previously incubated U937 cells using an RNA isolation kit (Zymo Research, Irvine, CA)

according to the manufacturer's instructions. RNA was converted to complimentary (c) DNA using Applied Biosystems' High-Capacity cDNA Reverse Transcription Kit (Foster City, CA). Gene-specific forward or reverse primers (0.2 μM; IDT, Coralville, IA), cDNA (2 μL/reaction), and SYBR Green nucleic acid staining dye (10 μL/reaction; Applied Biosystems) were used for qRT-PCR via a LightCycler LC480 Instrument (Roche Diagnostics, Indianapolis, IN). Gene expression was assessed using the ΔΔ-Ct method and standardized to the expression of the housekeeping gene, beta-actin (*ACTB*). Gene primers were designed using Primer3 primer design software (Untergasser et al., 2012). Primers in this study were detailed in Supplemental Table 2.

### 2.5. Statistical Analysis

Graphpad Prism 8.0 (GraphPad Software, Inc., La Jolla, CA) was used to perform one-way analysis of variance (ANOVA) and post hoc Tukey's tests for determinations of statistically significant, treatment-related, inter-group differences at a significance level of $p < 0.05$. Shapiro-Wilk tests were used to confirm normality and no data points were excluded. Data are expressed herein as mean ± standard error of the mean (SEM).

## 3. RESULTS

### 3.1. Chemical Characterization

All three PM extracts contained a wide range of elements detected by ICP-MS (Table 1). However, the elements in these PM extracts differed greatly in concentration. For example, the concentration of Cu was more than 17 times higher in $PM_{CA}$ compared to $PM_{SD}$ and $PM_{SX}$ at 2.13, 0.12, and 0.054 parts per million (ppm) of PM mass, respectively. Fe was also higher in $PM_{CA}$ compared to $PM_{SD}$ and $PM_{SX}$, although to a lesser degree (1.1, 0.34, and 0.66 ppm, respectively).

HR-AMS analysis revealed that $PM_{SX}$, $PM_{SD}$, and $PM_{CA}$ stock extracts consisted primarily of organic compounds (44%, 57%, and 54% of total mass, respectively). Despite the similar total organic content, fractions of carbon (C), oxygen (O), hydrogen (H), and nitrogen (N) were variable across the three extract samples (Table 3). $PM_{CA}$ was found to have the most oxidized organics (Table 2). Inorganic nitrate and sulfate contents were comparable in $PM_{SD}$ and $PM_{SX}$ with 4% and 12% differences, respectively; however, $PM_{SX}$ had more sulfate, while $PM_{SD}$ had more nitrate. In $PM_{CA}$, inorganic nitrate and sulfate comprised 32% and 2% of the total mass, respectively (Table 2).

### 3.2. BALF Analysis

Although $PM_{CA}$ appeared to produce greater numbers of total cells in exposed mice relative to other PM treatments, the only significant difference from CTRL was observed for $PM_{CA}$ on Day 2 (Figure 1A; $p = 0.0463$). In contrast, on Day 1, statistically significant increases in neutrophil numbers were found for all three PM extracts ($PM_{SX}$, $PM_{SD}$ and $PM_{CA}$), compared to CTRL (Figure 1B; $p$=0.0232, 0.0357 and 0.0114, respectively), $PM_{CA}$ increased significantly neutrophil numbers than $PM_{SX}$ and $PM_{SD}$ as well (Figure 1B; $p$=0.0225 and 0.0378, respectively). A slight, increase in neutrophil numbers was seen from Day 1 to 2 in mice exposed to $PM_{SX}$, but this increase did not achieve a level of statistical

significance. While neutrophilia in mice exposed to $PM_{SD}$ and $PM_{CA}$ appeared to be resolving over the same time frame (Figure 1B), those exposed to $PM_{SX}$ and $PM_{CA}$ continued to show significant differences from controls at Day 2 (Figure 1B; $p = 0.0358$ and 0.0027, respectively). By Day 4, neutrophil counts for all three groups of mice exposed to PM had returned to control levels. No statistically significant differences were noted in macrophage counts at any day post-OPA (Figure 1C).

### 3.3. Histological Analysis of Lung Tissues

Bronchiolar inflammation was significantly observed only on Day 1, when all PM-exposed groups appeared to exhibit elevated responses compared to controls (Figure 2A). However, of the three groups, only mice exposed to $PM_{SX}$ or $PM_{CA}$ had significantly higher bronchiolitis scores relative to controls (Figure 2A; $p = 0.0096$ and $p = 0.0045$, respectively), those administered $PM_{SX}$ or $PM_{CA}$ demonstrated the most severe bronchiolar effects, with inflammatory cell influx to the lungs in peribronchiolar regions (Figure 3A–D). By Days 2 and 4, no notable inter-group differences were observed (Figure 2A).

Semi-quantitative histopathological scoring demonstrated significantly greater alveolitis on Day 1 in mice exposed to $PM_{SX}$ versus CTRL (Figure 2B; $p = 0.0436$). Alveolitis was evident in the form of greater numbers of macrophages and neutrophils in the alveoli of mice exposed to $PM_{SX}$ compared to CTRL (Figures 4A versus 4B). By Day 2 and 4, alveolar inflammation appeared to resolve (Figure 2B). $PM_{SX}$-exposed mice also demonstrated perivascular inflammation to a statistically significant degree compared to control mice, as well as $PM_{SD}$-exposed mice on Day 1 (Figure 2C; $p = 0.0137$ and $p = 0.0349$, respectively). By Days 2 and 4, no notable inter-group differences were observed (Figure 2C).

### 3.4 DRE Luciferase Reporter Assay

The DRE-luciferase reporter activities of PM extracts were significantly ($p < 0.0001$) greater than DMSO suggesting the tested PM, irrespective of the source, was highly effective at activating the AhR in stable transfected HepG2 cells (Figure 5). $PM_{SX}$ was a more potent activator than $PM_{SD}$ and $PM_{CA}$ ($p < 0.0001$ for both), at a slightly greater (non-significant) level of activation than that induced by B[a]P (Figure 5). In fact, the AhR activities induced by $PM_{SD}$ and $PM_{CA}$ were each less than 50% of that induced by $PM_{SX}$ (Figure 5). Overall, the luciferase assay results suggested all of the tested PM extracts were capable of activating the AhR, a process plausibly attributable to binding of unidentified PAHs to AhR in each of the PM samples. Because $PM_{SX}$ induced AhR activity comparable to that of the standard PAHs reference material, B[a]P, the observed induction was probably due to more potent and abundant PAHs in $PM_{SX}$ versus $PM_{SD}$ and $PM_{CA}$ (Figure 5).

### 3.5 Gene expression

In general, expression of *CYP1A1*, *COX-2*, *IL-8,* and *IL-1β* genes was highest in U937 cells incubated for 6, 24, or 48 hours with $PM_{SX}$ versus DMSO, $PM_{SD}$, or $PM_{CA}$ ($p<0.05$; Figures 6–7). Gene induction appeared to peak after 24 hours of cell incubation with $PM_{SX}$ versus DMSO ($p<0.05$; Figure 6). This was particularly true for *CYP1A1* and *COX-2* genes,

with associated mRNA levels elevated 36-fold and 5-fold, respectively, in $PM_{SX}$-exposed mice versus their control counterparts.

## 4. DISCUSSION

Sun *et al.* (2017) also compared the acute, inflammatory effects of $PM_{SX}$ and $PM_{CA}$. In their study, OPA was performed once, with each mouse given 50 μL of either Milli-Q water (vehicle control) or a 1 mg/mL PM extract ($PM_{SX}$ or $PM_{CA}$), and necropsied 24 hours later. Their results demonstrated $PM_{CA}$ produced significantly ($p < 0.05$) higher levels of BALF neutrophils, histopathologic scores, and protein levels than $PM_{SX}$ (Sun et al., 2017). In the present study, we tested the same sham control and PM extract samples as Sun *et al.*(2017), in addition to $PM_{SD}$. The same OPA administration procedures were performed, but in the present study, time-lag effects were observed over three post-OPA days (Days 1, 2, and 4). Interestingly, at Day 1, although $PM_{CA}$ significantly increased BALF neutrophil numbers compared to control, $PM_{SX}$ and $PM_{SD}$ (Figure 1B), $PM_{SX}$ produced a more prominent tissue inflammation response than $PM_{CA}$ (Figure 2A–C). Therefore, *In vitro* experiments were included in the present study to further investigate the molecular mechanisms driving these findings.

Activated neutrophils play a key role in the development of acute lung injury. In experimental models of acute lung injury, neutrophils that accumulate in the lungs are associated with increased levels of pro-inflammatory cytokines (Abraham, 2003). In our previous study (Sun et al., 2017), $PM_{CA}$ induced pulmonary inflammation observed as neutrophilia in BALF and increased levels of chemokines involved in neutrophil recruitment to the lungs. Van Winkle *et al.* (2015) have shown similar findings. In the present study, $PM_{CA}$ again induced the highest number of BALF neutrophils when compared to control, $PM_{SX}$ and $PM_{SD}$ at 1-day post-OPA (Figure 1B; $p$=0.0114, 0.0225 and 0.0378, respectively). It is interesting to note statistically significant differences in neutrophilia were apparent at 2 days post-OPA for both $PM_{CA}$ and $PM_{SX}$ compared to control (Figure 1B; $p$ = 0.0358 and 0.0027). However, by Day 4, neutrophil was completely attenuated, suggesting recovery from the acute lung injury observed at earlier post-OPA Days 1 and 2 (Figure 1B). These findings also strongly suggested each PM extract induced different degrees and patterns of inflammation following exposure.

Using an unbiased, semi-quantitative histopathology rubric, we observed that $PM_{SX}$ exposure led to statistically significant increases in bronchiolar, alveolar and perivascular lung inflammation relative to CTRL at post-OPA Day 1 (Figures 2A–C; p=0.0096, 0.0436 *and* 0.0137, respectively). Alteration of the matrisome through successive damage and repair of the extracellular matrix can induce inflammatory lung conditions. In such a dysregulated state, excess production of an abnormal or pathological matrix can contribute to the accumulation of macrophages in the airways and the alveoli (Kaur et al., 2015), thus stimulating circulating neutrophils and monocytes (precursors of macrophages) to enter the air spaces and signal an acute respiratory inflammatory response(Perry et al., 1993). As shown in Figures 3 and 4, there were numerous macrophages in the peribronchiolar region and alveolar lumen following exposure to $PM_{SX}$. However, some of the inflammatory patterns observed in tissues were not reflected in BAL neutrophil counts. These differences

prompted us to perform *in vitro* experiments to further study the role of macrophages in mediating effects of acute $PM_{SX}$, $PM_{SD}$, or $PM_{CA}$ exposure.

Depending on the source, PM may be composed of mixtures of inorganic compounds, trace elements, elemental carbon, and an exhaustive list of organic compounds, including PAHs. The biological role of metals and oxidative organics in each PM extract could not be clearly defined; however, clear compositional differences are evident among the extracts to provide plausible biological effects of action. PAHs have received considerable attention due to their potential toxic, carcinogenic, and mutagenic effects. They are also predominant factors in the activation of AhR by PM (Castaneda et al., 2017; Zhang et al., 2016). As a cytosolic receptor protein, the AhR binds a diverse array of ligands, which may impact the immune system depending on the binding duration, route of exposure, and cytokine milieu (Julliard et al., 2014). In the current study, all three PM extracts significantly activated the AhR relative to control (Figure 4; $p<0.0001$), but $PM_{SX}$ was especially potent. This latter point may be explained by the fact that coal combustion was a major source of $PM_{SX}$. Coal consumption in China in 2012 reached 2.75 billion tons of standard coal (tce), approximately one-half of the global coal consumption, and Shanxi province is one of the largest coal production centers in China (Yang and Teng, 2018). Coal combustion produces gaseous pollutants and PM, often containing toxic components such as heavy metals and PAHs (Shen et al., 2010). Although, in the present study, we were unable to definitively identify the chemical constituent(s) responsible for the observed biological effects, we know PAHs were likely present in all three PM samples as contributors to the differential gene induction effects. A previous study by Zhang *et al*. (2016) identified multiple PAHs in $PM_{SX}$, with benzo(b)fluoranthene (B[b]F), benzo(e)pyrene (B[e]P), and benzo(a)pyrene (B[a]P) predominant. Therefore, the greater level of AhR activation (observed as DRE luciferase units) produced by $PM_{SX}$ relative to $PM_{SD}$ and $PM_{CA}$ (Figure 5) suggests $PM_{SX}$ contains a greater PAH concentration and/or more potent PAHs than the other two PM extracts.

Vogel and colleagues have shown the transfection efficiency for HepG2 cells is superior to that of human U937 cells for the luciferase assay test. The AhR expression level in HepG2 cells is approximately 20 times compared to U937 cells (Vogel et al., 2019). Human U937 cells have been shown to be a suitable cell type to identify inflammatory responses following exposure to ambient PM from urban dust or diesel exhaust PM (Vogel et al., 2005). In the current study, all PM extracts induced expression of the AhR-regulated downstream gene, *CYP1A1*, as well as genes for molecular markers of inflammation (*COX-2*, *IL-8*, and *IL-1β*) in human U937 macrophages (Figures 6 and 7; $p<0.05$). PM appeared to activate the greatest inflammatory responses *in vitro* at 24 hours compared to 6 and 48 hours. Interestingly, $PM_{SX}$ was the most effective activator of AhR, and it was significantly more effective at inducing *CYP1A1*, *COX-2*, *IL-8*, and *IL-1β* genes than $PM_{SD}$ and $PM_{CA}$, thus highlighting the critical role of AhR in the observed PM-mediated inflammatory responses. The specific mechanisms by which this activation occurred remains unclear beyond simple PAHs stimulation.

## 5. CONCLUSIONS

In the present study, a single OPA exposure was used to test the in vivo toxicity of each PM sample in mice. Though exposures did not occur by inhalation, OPA was the most effective method to simulate inhalation of equal masses of the various PM samples collected from diverse geographic locations for comparison. Repeat exposures were not performed; however, results indicated a single OPA exposure to any of the tested PM extracts could induce transient and acute inflammation, with the greatest *in vivo* responses produced by $PM_{CA}$ and $PM_{SX}$ at Day 1, and attenuation of effects in all PM-exposed groups at Day 4. A striking finding was the clear differential *in vitro* activation of the AhR for each of the three PM extracts in human U937 macrophages. These findings, as well as the differential activation of other cytokines by macrophages, provides new observations that may give rise to better understanding PM effects *in vivo* and at the cellular level. The time-lag effects of PM with varied PM chemical composition may play a critical role in the overall process of injury and repair.

## Supplementary Material

Refer to Web version on PubMed Central for supplementary material.

## ACKNOWLEDGEMENTS

The authors thank Katarina Gradin (Karolinska Institute, Stockholm, Sweden) for providing HepG2 cells stable transfected with PTX.DIR containing a DRE luciferase reporter construct. The technical assistance of Dale Uyeminami, Tiffany Mar and Dr. Liangliang Cui, as well as the editorial assistance of Dr. Rona Silva are appreciated.

6. FUNDING

This work was supported in part by the National Institute of Occupational Safety and Health research grant U54 OH07550 (KEP), the National Institute of Environmental Health Sciences research grants R01 ES029126 (CFV) and P30 ES023513 (KEP) and P51 OD011107 (KEP).

## References

Abraham E, 2003 Neutrophils and acute lung injury. Crit Care Med 31, S195–199.

Aggarwal NR, King LS, D'Alessio FR, 2014 Diverse macrophage populations mediate acute lung inflammation and resolution. Am J Physiol Lung Cell Mol Physiol 306, L709–725.

Aiken AC, Decarlo PF, Kroll JH, Worsnop DR, Huffman JA, Docherty KS, Ulbrich IM, Mohr C, Kimmel JR, Sueper D, Sun Y, Zhang Q, Trimborn A, Northway M, Ziemann PJ, Canagaratna MR, Onasch TB, Alfarra MR, Prevot AS, Dommen J, Duplissy J, Metzger A, Baltensperger U, Jimenez JL, 2008 O/C and OM/OC ratios of primary, secondary, and ambient organic aerosols with high-resolution time-of-flight aerosol mass spectrometry. Environ Sci Technol 42, 4478–4485. [PubMed: 18605574]

Bein KJ, Wexler AS, 2015 Compositional variance in extracted particulate matter using different filter extraction techniques. Atmospheric Environment 107, 24–34.

Berghard A, Gradin K, Pongratz I, Whitelaw M, Poellinger L, 1993 Cross-coupling of signal transduction pathways: the dioxin receptor mediates induction of cytochrome P-4501A1 expression via a protein kinase C-dependent mechanism. Mol Cell Biol 13, 677–689. [PubMed: 8380231]

Byrne AJ, Mathie SA, Gregory LG, Lloyd CM, 2015 Pulmonary macrophages: key players in the innate defence of the airways. Thorax 70, 1189–1196. [PubMed: 26286722]

Canagaratna MR, Jayne JT, Jimenez JL, Allan JD, Alfarra MR, Zhang Q, Onasch TB, Drewnick F, Coe H, Middlebrook A, Delia A, Williams LR, Trimborn AM, Northway MJ, DeCarlo PF, Kolb CE, Davidovits P, Worsnop DR, 2007 Chemical and microphysical characterization of ambient aerosols with the aerodyne aerosol mass spectrometer. Mass Spectrom Rev 26, 185–222. [PubMed: 17230437]

Castaneda AR, Bein KJ, Smiley-Jewell S, Pinkerton KE, 2017 Fine particulate matter (PM2.5) enhances allergic sensitization in BALB/c mice. J Toxicol Environ Health A 80, 197–207. [PubMed: 28494199]

Chan KS, Roberts E, McCleary R, Buttorff C, Gaskin DJ, 2014 Community characteristics and mortality: the relative strength of association of different community characteristics. Am J Public Health 104, 1751–1758. [PubMed: 25033152]

Craig L, Brook JR, Chiotti Q, Croes B, Gower S, Hedley A, Krewski D, Krupnick A, Krzyzanowski M, Moran MD, Pennell W, Samet JM, Schneider J, Shortreed J, Williams M, 2008 Air pollution and public health: a guidance document for risk managers. J Toxicol Environ Health A 71, 588–698. [PubMed: 18569631]

Di Filippo P, Riccardi C, Gariazzo C, Incoronato F, Pomata D, Spicaglia S, Cecinato A, 2007 Air pollutants and the characterization of the organic content of aerosol particles in a mixed industrial/semi-rural area in central Italy. J Environ Monit 9, 275–282. [PubMed: 17344954]

Gunasekar PG, Stanek LW, 2011 Advances in exposure and toxicity assessment of particulate matter: an overview of presentations at the 2009 Toxicology and Risk Assessment Conference. Toxicol Appl Pharmacol 254, 141–144. [PubMed: 21034760]

Hawk ET, Viner JL, Dannenberg A, DuBois RN, 2002 COX-2 in cancer--a player that's defining the rules. J Natl Cancer Inst 94, 545–546. [PubMed: 11959883]

Holmes HA, Sriramasamudram JK, Pardyjak ER, Whiteman CD, 2015 Turbulent fluxes and pollutant mixing during wintertime air pollution episodes in complex terrain. Environ Sci Technol 49, 13206–13214.

Julliard W, Fechner JH, Mezrich JD, 2014 The aryl hydrocarbon receptor meets immunology: friend or foe? A little of both. Front Immunol 5, 458. [PubMed: 25324842]

Kaur M, Bell T, Salek-Ardakani S, Hussell T, 2015 Macrophage adaptation in airway inflammatory resolution. Eur Respir Rev 24, 510–515. [PubMed: 26324813]

Kelly FJ, Fussell JC, 2012 Size, source and chemical composition as determinants of toxicity attributable to ambient particulate matter. Atmospheric Environment 60, 504–526.

Krewski D, Burnett R, Jerrett M, Pope CA, Rainham D, Calle E, Thurston G, Thun M, 2005 Mortality and long-term exposure to ambient air pollution: ongoing analyses based on the American Cancer Society cohort. J Toxicol Environ Health A 68, 1093–1109. [PubMed: 16024490]

Laurent O, Hu J, Li L, Kleeman MJ, Bartell SM, Cockburn M, Escobedo L, Wu J, 2016 Low birth weight and air pollution in California: Which sources and components drive the risk? Environ Int 92-93, 471–477.

Mathiesen M, Pedersen EK, Bjorseth O, Egeberg KW, Syversen T, 2004 Heating of indoor dust causes reduction in its ability to stimulate release of IL-8 and TNFalpha in vitro compared to non-heated dust. Indoor Air 14, 226–234. [PubMed: 15217476]

Okey AB, 2007 An aryl hydrocarbon receptor odyssey to the shores of toxicology: the Deichmann Lecture, International Congress of Toxicology-XI. Toxicol Sci 98, 5–38. [PubMed: 17569696]

Perry VH, Andersson PB, Gordon S, 1993 Macrophages and inflammation in the central nervous system. Trends Neurosci 16, 268–273. [PubMed: 7689770]

Pinkerton KE, Chen CY, Mack SM, Upadhyay P, Wu CW, Yuan W, 2019 Cardiopulmonary health effects of airborne particulate matter: correlating animal toxicology to human epidemiology. Toxicol Pathol 47, 954–961. [PubMed: 31645209]

Pinkerton KE, Green FHY, Saiki C, Vallyathan V, Plopper CG, Gopal V, Hung D, Bahne EB, Lin SS, Menache MG, Schenker MB, 2000 Distribution of particulate matter and tissue remodeling in the human lung. Environmental Health Perspectives 108, 1063–1069. [PubMed: 11102298]

Shen G, Wang W, Yang Y, Zhu C, Min Y, Xue M, Ding J, Li W, Wang B, Shen H, Wang R, Wang X, Tao S, 2010 Emission factors and particulate matter size distribution of polycyclic aromatic

hydrocarbons from residential coal combustions in rural Northern China. Atmospheric Environment 44, 5237–5243.

Silva RM, Doudrick K, Franzi LM, Teesy C, Anderson DS, Wu ZQ, Mitra S, Vu V, Dutrow G, Evans JE, Westerhoff P, Van Winkle LS, Raabe OG, Pinkerton KE, 2014 Instillation versus inhalation of multiwalled carbon nanotubes: exposure-related health effects, clearance, and the role of particle characteristics. Acs Nano 8, 8911–8931. [PubMed: 25144856]

Silva RM, Teesy C, Franzi L, Weir A, Westerhoff P, Evans JE, Pinkerton KE, 2013 Biological response to nano-scale titanium dioxide (TiO2): role of particle dose, shape, and retention. J Toxicol Environ Health A 76, 953–972. [PubMed: 24156719]

Smith KR, Kim S, Recendez JJ, Teague SV, Menache MG, Grubbs DE, Sioutas C, Pinkerton KE, 2003 Airborne particles of the california central valley alter the lungs of healthy adult rats. Environ Health Perspect 111, 902–908; discussion A408–909. [PubMed: 12782490]

Sun X, Wei H, Young DE, Bein KJ, Smiley-Jewell SM, Zhang Q, Fulgar CCB, Castaneda AR, Pham AK, Li W, Pinkerton KE, 2017 Differential pulmonary effects of wintertime California and China particulate matter in healthy young mice. Toxicol Lett 278, 1–8. [PubMed: 28698096]

Sun Y, Zhang Q, Zheng M, Ding X, Edgerton ES, Wang X, 2011 Characterization and source apportionment of water-soluble organic matter in atmospheric fine particles (PM2.5) with high-resolution aerosol mass spectrometry and GC-MS. Environ Sci Technol 45, 4854–4861. [PubMed: 21539378]

Suwa T, Hogg JC, Quinlan KB, Ohgami A, Vincent R, van Eeden SF, 2002 Particulate air pollution induces progression of atherosclerosis. Journal of the American College of Cardiology 39, 935–942. [PubMed: 11897432]

Tang D, Wang C, Nie J, Chen R, Niu Q, Kan H, Chen B, Perera F, Taiyuan CDC, 2014 Health benefits of improving air quality in Taiyuan, China. Environ Int 73, 235–242. [PubMed: 25168129]

Untergasser A, Cutcutache I, Koressaar T, Ye J, Faircloth BC, Remm M, Rozen SG, 2012 Primer3--new capabilities and interfaces. Nucleic Acids Res 40, e115.

Van Winkle LS, Bein K, Anderson D, Pinkerton KE, Tablin F, Wilson D, Wexler AS, 2015 Biological dose response to PM2.5: effect of particle extraction method on platelet and lung responses. Toxicol Sci 143, 349–359. [PubMed: 25389146]

Vogel CF, Garcia J, Wu D, Mitchell DC, Zhang Y, Kado NY, Wong P, Trujillo DA, Lollies A, Bennet D, Schenker MB, Mitloehner FM, 2012 Activation of inflammatory responses in human U937 macrophages by particulate matter collected from dairy farms: an in vitro expression analysis of pro-inflammatory markers. Environ Health 11, 17. [PubMed: 22452745]

Vogel CF, Li W, Sciullo E, Newman J, Hammock B, Reader JR, Tuscano J, Matsumura F, 2007 Pathogenesis of aryl hydrocarbon receptor-mediated development of lymphoma is associated with increased cyclooxygenase-2 expression. Am J Pathol 171, 1538–1548. [PubMed: 17823287]

Vogel CF, Sciullo E, Wong P, Kuzmicky P, Kado N, Matsumura F, 2005 Induction of proinflammatory cytokines and C-reactive protein in human macrophage cell line U937 exposed to air pollution particulates. Environ Health Perspect 113, 1536–1541. [PubMed: 16263508]

Vogel CFA, Kado SY, Kobayashi R, Liu X, Wong P, Na K, Durbin T, Okamoto RA, Kado NY, 2019 Inflammatory marker and aryl hydrocarbon receptor-dependent responses in human macrophages exposed to emissions from biodiesel fuels. Chemosphere 220, 993–1002. [PubMed: 31543100]

WHO, 2018 Ambient (outdoor) air quality and health. World Health Organization, https://www.who.int/news-room/fact-sheets/detail/ambient-(outdoor)-air-quality-and-health.

Yang X, Teng F, 2018 The air quality co-benefit of coal control strategy in China. Resources, Conservation and Recycling 129, 373–382.

Zhang J, Fulgar CC, Mar T, Young DE, Zhang Q, Bein KJ, Cui L, Castaneda A, Vogel CFA, Sun X, Li W, Smiley-Jewell S, Zhang Z, Pinkerton KE, 2018 TH17-Induced neutrophils enhance the pulmonary allergic response following BALB/c exposure to house dust mite allergen and fine particulate matter from California and China. Toxicol Sci 164, 627–643. [PubMed: 29846732]

Zhang J, Liu Y, Cui LL, Liu SQ, Yin XX, Li HC, 2017 Ambient air pollution, smog episodes and mortality in Jinan, China. Sci Rep 7, 11209.

Zhang M, Xie J, Wang Z, Zhao L, Zhang H, Li M, 2016 Determination and source identification of priority polycyclic aromatic hydrocarbons in PM2.5 in Taiyuan, China. Atmospheric Research 178-179, 401–414.

## Highlights

1. Time lag effects following an acute exposure to three PM samples were evaluated.
2. All three PM samples induced acute, but transient inflammation in the lungs of mice.
3. All three PM samples induced AhR and inflammatory gene expression in human U937 cells.
4. Time lag effects for PM samples may play critical roles in PM-induced injury and repair.

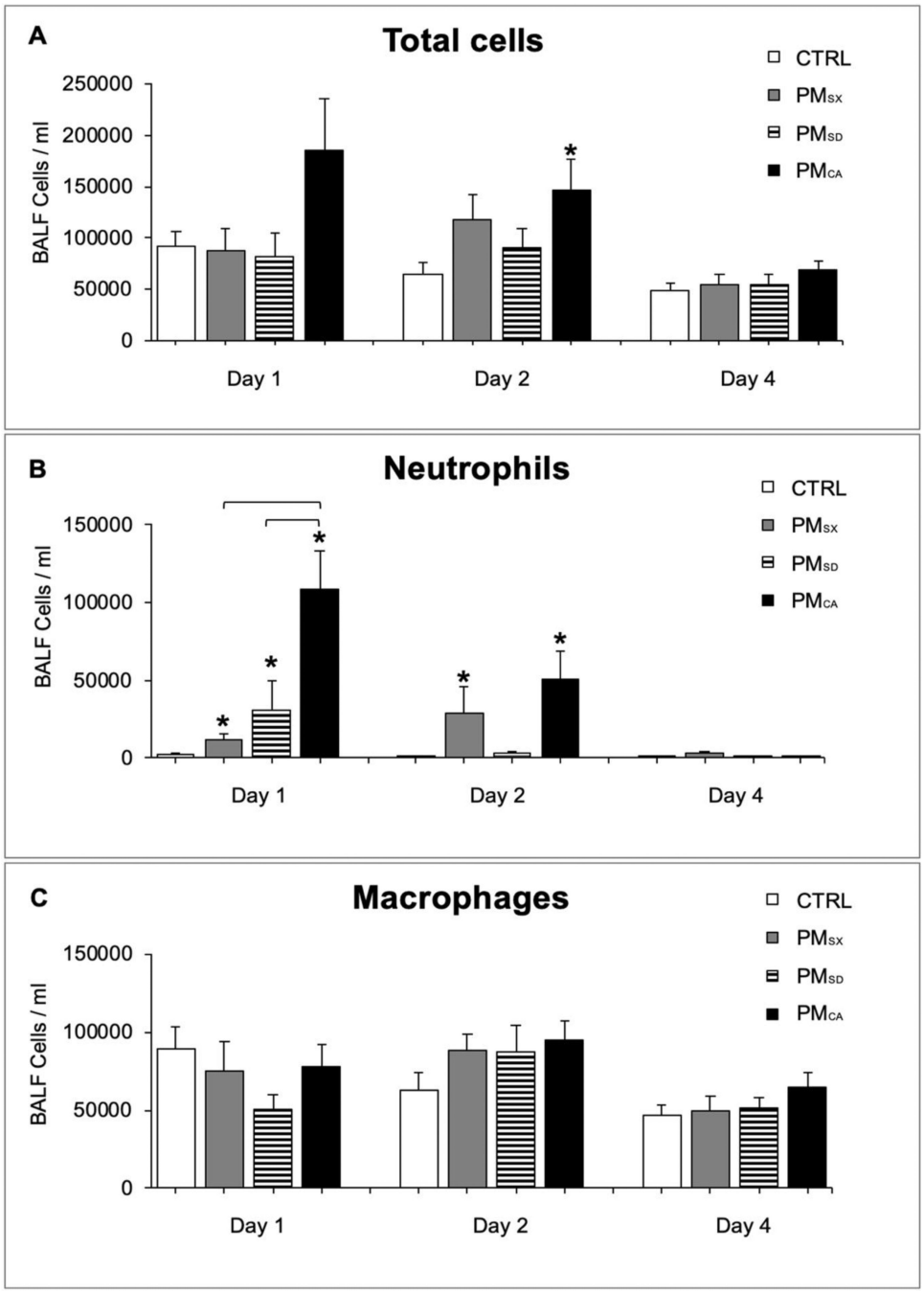


**Figure 1. Particulate matter (PM) extracts from California produced more inflammatory responses in bronchoalveolar lavage fluid (BALF) than those from China.**

Total cell (A), neutrophil (B), and macrophage (C) counts are shown for mice exposed to Milli-Q water vehicle control (CTRL) or particulate matter extracts from Taiyuan, Shanxi ($PM_{SX}$); Jinan, Shandong ($PM_{SD}$); or Sacramento, California ($PM_{CA}$), and sacrificed 1, 2, or 4 days post exposure. Data are presented as the mean ± standard error of the mean. * indicates a significant ($p < 0.05$) difference from controls. Brackets indicate significant ($p < 0.05$) differences between noncontrol groups. N = 18/group (6/group/necropsy day).

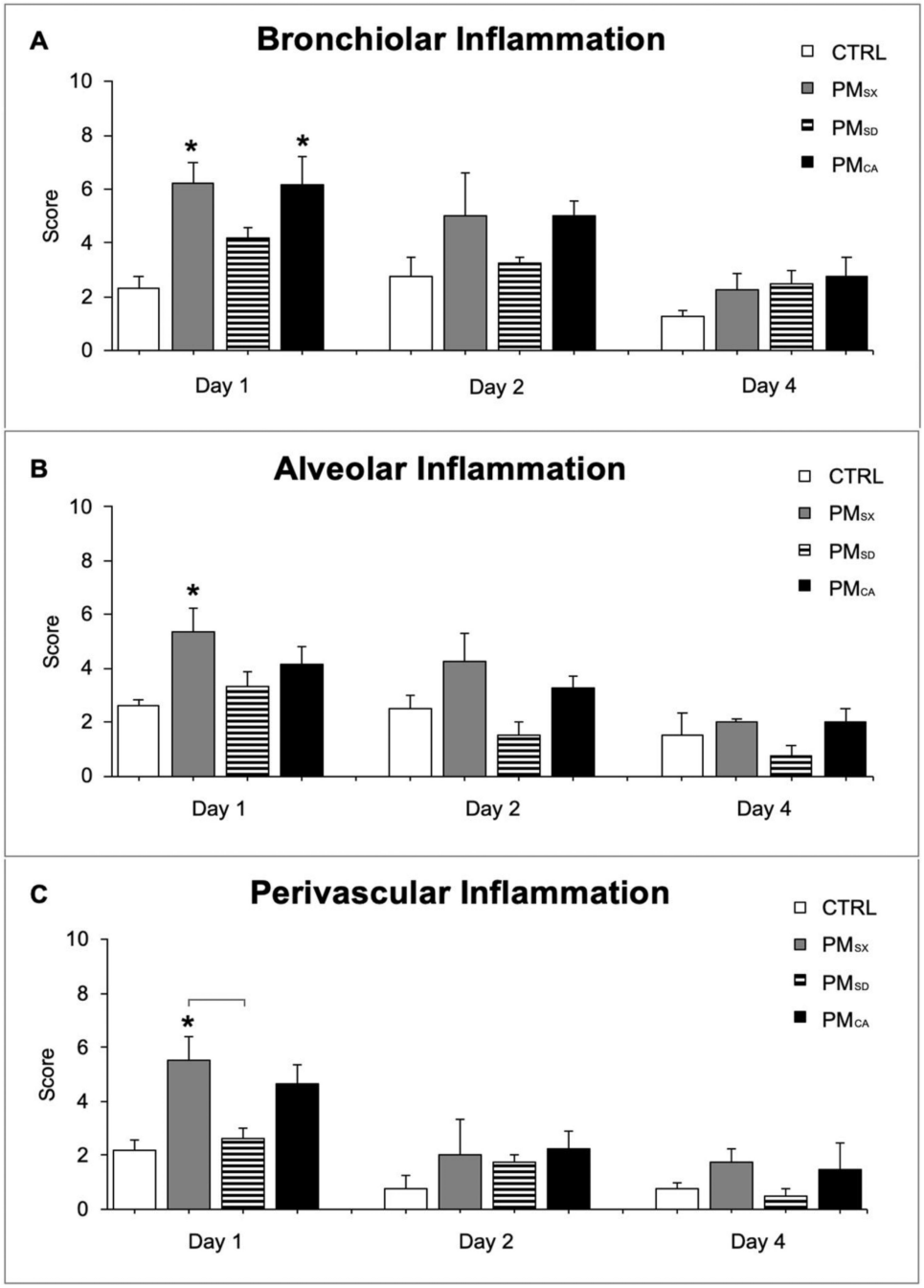


**Figure 2. Particulate matter extract samples from Shanxi, China ($PM_{SX}$) produced more histopathologic lung inflammation in mice.**

Graphs show semi-quantitative histopathology scores from the bronchiolar (A), alveolar (B), and perivascular (C) lung regions of mice exposed to Milli-Q water vehicle control (CTRL), or PM extracts from Taiyuan, Shanxi ($PM_{SX}$); Jinan, Shandong ($PM_{SD}$); or Sacramento, CA ($PM_{CA}$), and necropsied 1, 2, or 4 days thereafter. Data are mean ± standard error of the mean. * indicates a significant ($p < 0.05$) difference from controls. Brackets indicate significant ($p < 0.05$) differences between groups. N = 18 mice/PM exposed group (6 mice/group/necropsy day).

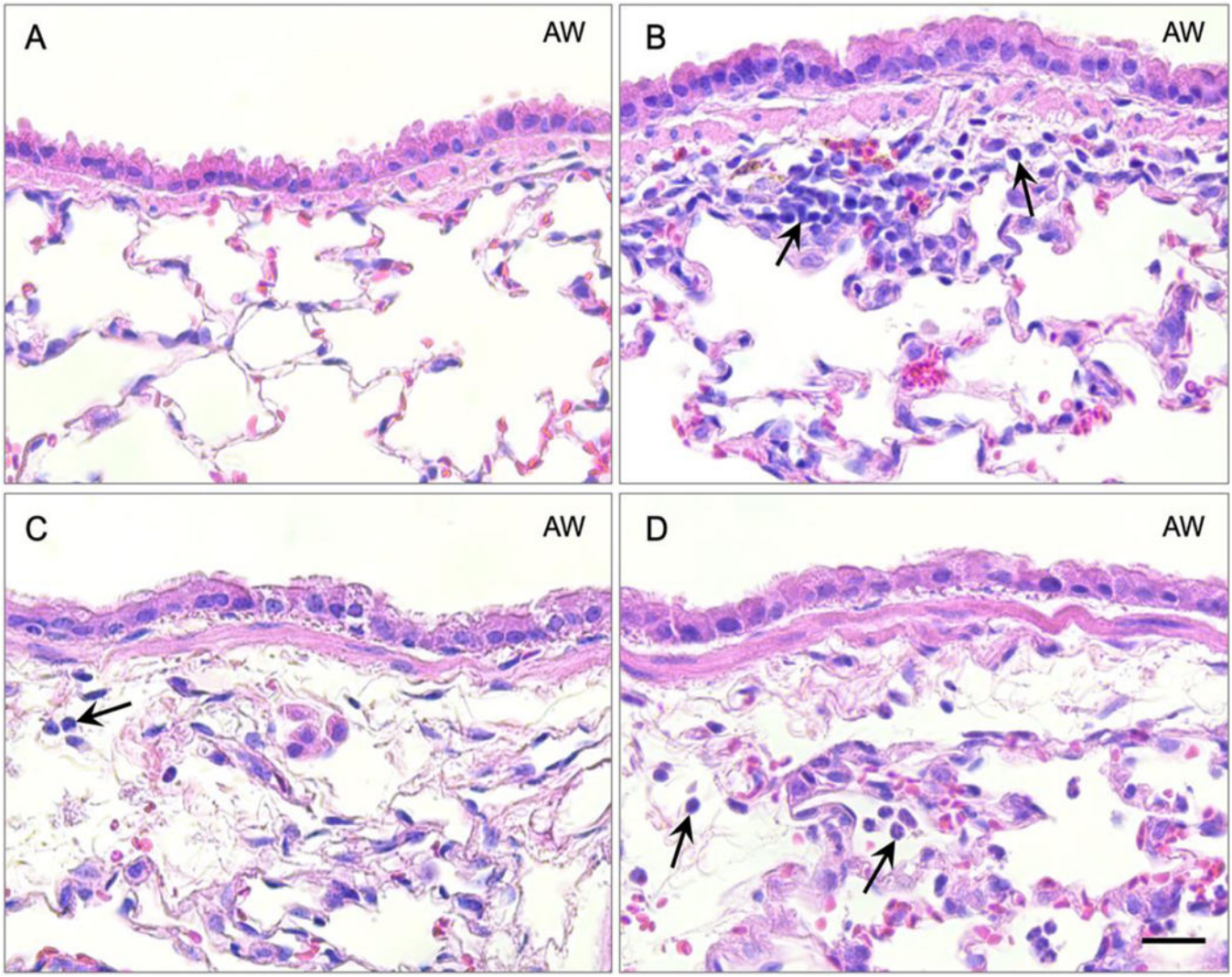


**Figure 3. Particulate matter (PM) extracts from China and California produced peribronchiolar inflammation in exposed mice.**

Panels are light micrographs of hematoxylin and eosin-stained mouse lung tissues collected one day after oropharyngeal aspiration of Milli-Q water (A) or PM extracts from Taiyuan, China (B); Jinan, China (C); or Sacramento, CA (D). Arrows pinpoint peribronchiolar inflammation. Scale bar is 20 μm. N = 18 mice/group (6 mice/group/necropsy day).

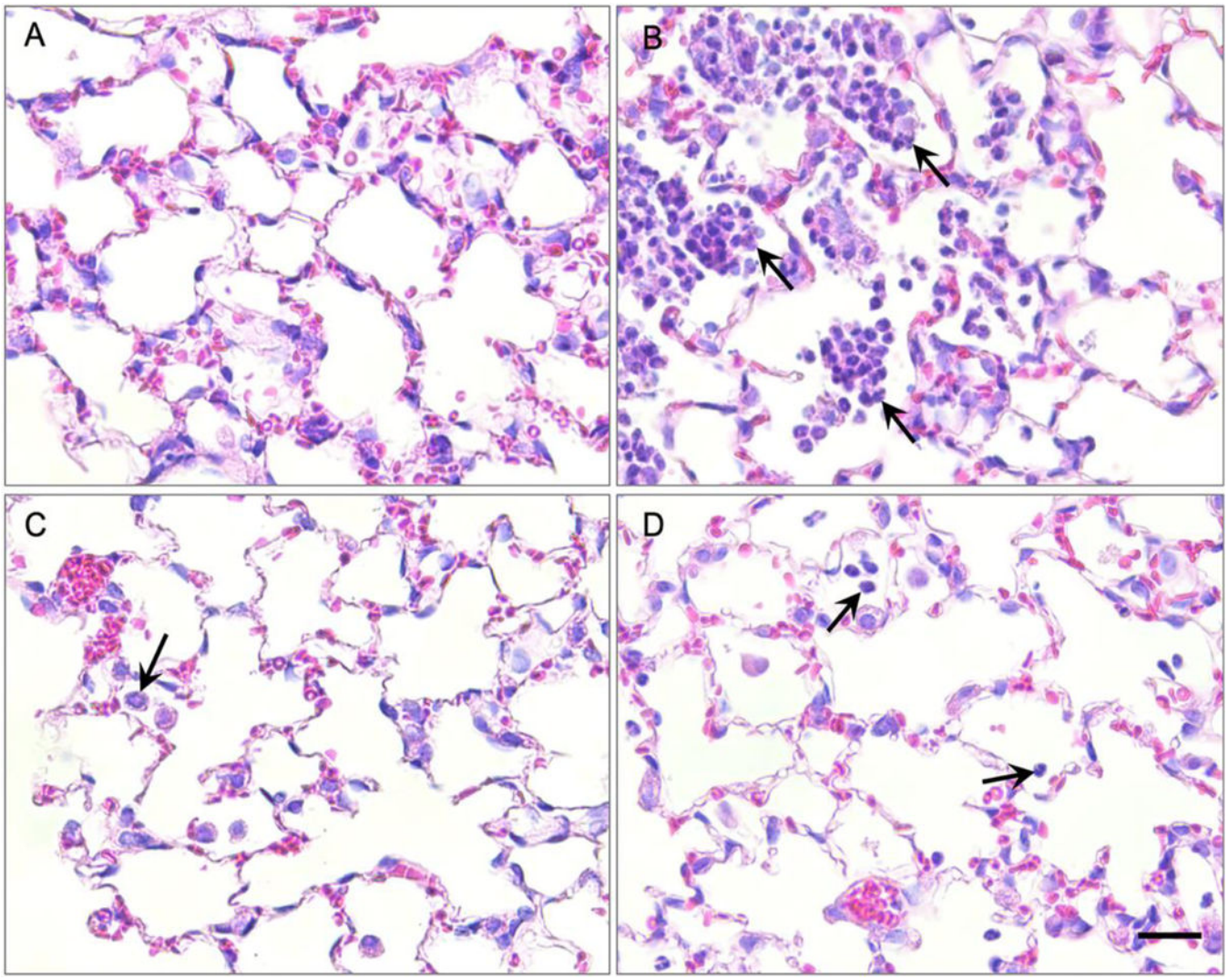


**Figure 4. Particulate matter (PM) extracts from China and California produced macrophagic alveolitis in exposed mice.**

Panels are light micrographs of hematoxylin and eosin-stained lung mouse tissues collected one day after oropharyngeal aspiration of Milli-Q water (vehicle control; A) or PM extracts from Taiyuan, China (B); Jinan, China (C); or Sacramento, CA (D). Arrows pinpoint alveolar inflammation. Scale bar is 20 μm. N = 18/group (6/group/necropsy day).

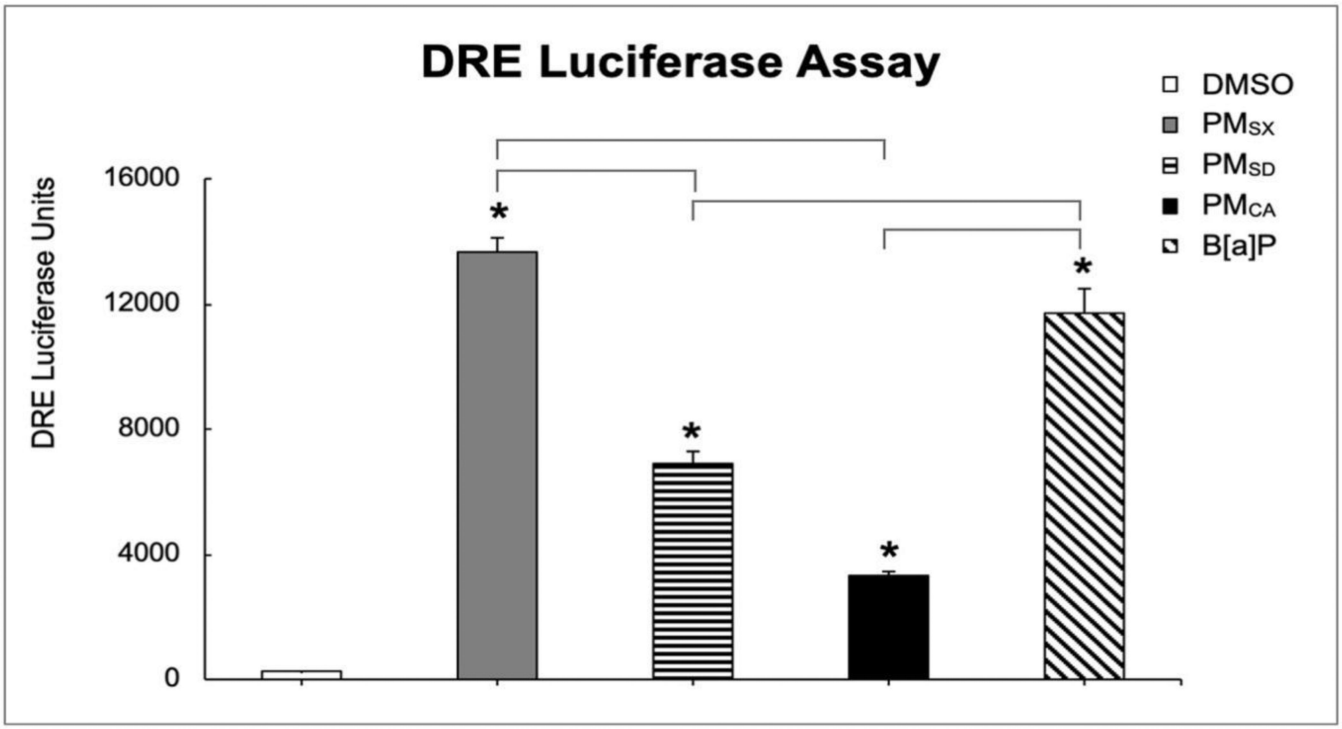


**Figure 5. Of the three PM extracts, $PM_{SX}$ induced the greatest dioxin-responsive element (DRE) luciferase reporter activity in HepG2 cells.**

This activity corresponded to aryl hydrocarbon receptor activation in cells incubated with DMSO (control); PM extracts from Taiyuan, Shanxi ($PM_{SX}$); Jinan, Shandong ($PM_{SD}$); or Sacramento, CA ($PM_{CA}$); or benzo(a)pyrene (B[a]P). Data are shown as mean ± SEM from experiments performed in triplicate. * indicates a significant difference ($p < 0.05$) from control. Brackets indicate significant ($p < 0.05$) differences between non-control groups.

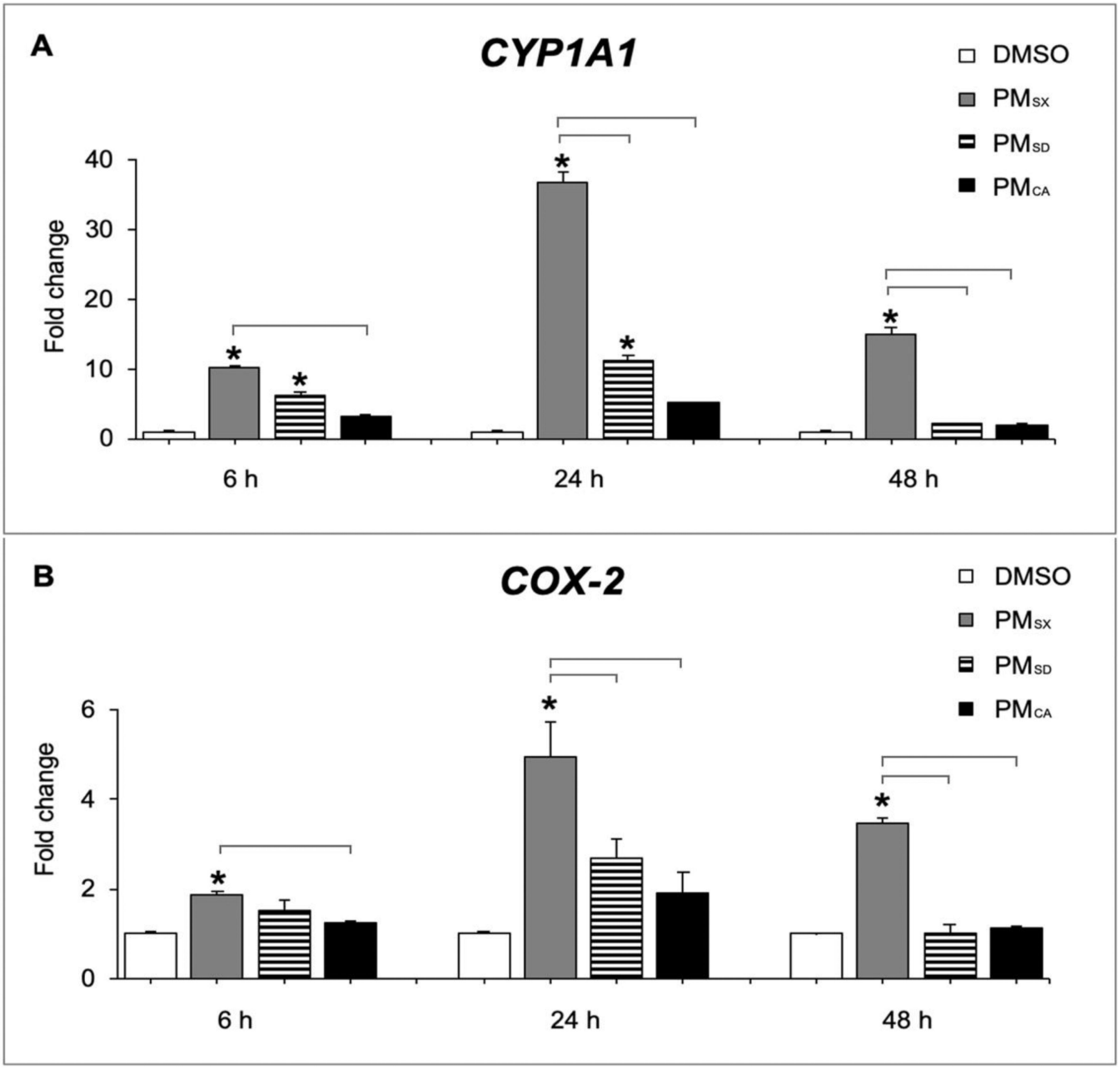


**Figure 6. $PM_{SX}$ significantly increased *CYP1A1* and *COX-2* mRNA levels in U937 macrophages following 6, 24, or 48 hours of exposure.**

Graphs show results from qPCR analysis of cells treated with DMSO (control), PM extracts from Taiyuan, Shanxi ($PM_{SX}$); Jinan, Shandong ($PM_{SD}$); or Sacramento, CA ($PM_{CA}$) for 6, 24, or 48 hours. Gene expression is shown as a fold-change from expression of the housekeeping gene, *ACTB* (beta-actin). Data are shown as mean ± SEM from experiments performed in triplicate. * indicates a significant difference ($p < 0.05$) from control. Brackets indicate significant ($p < 0.05$) differences between non-control groups.

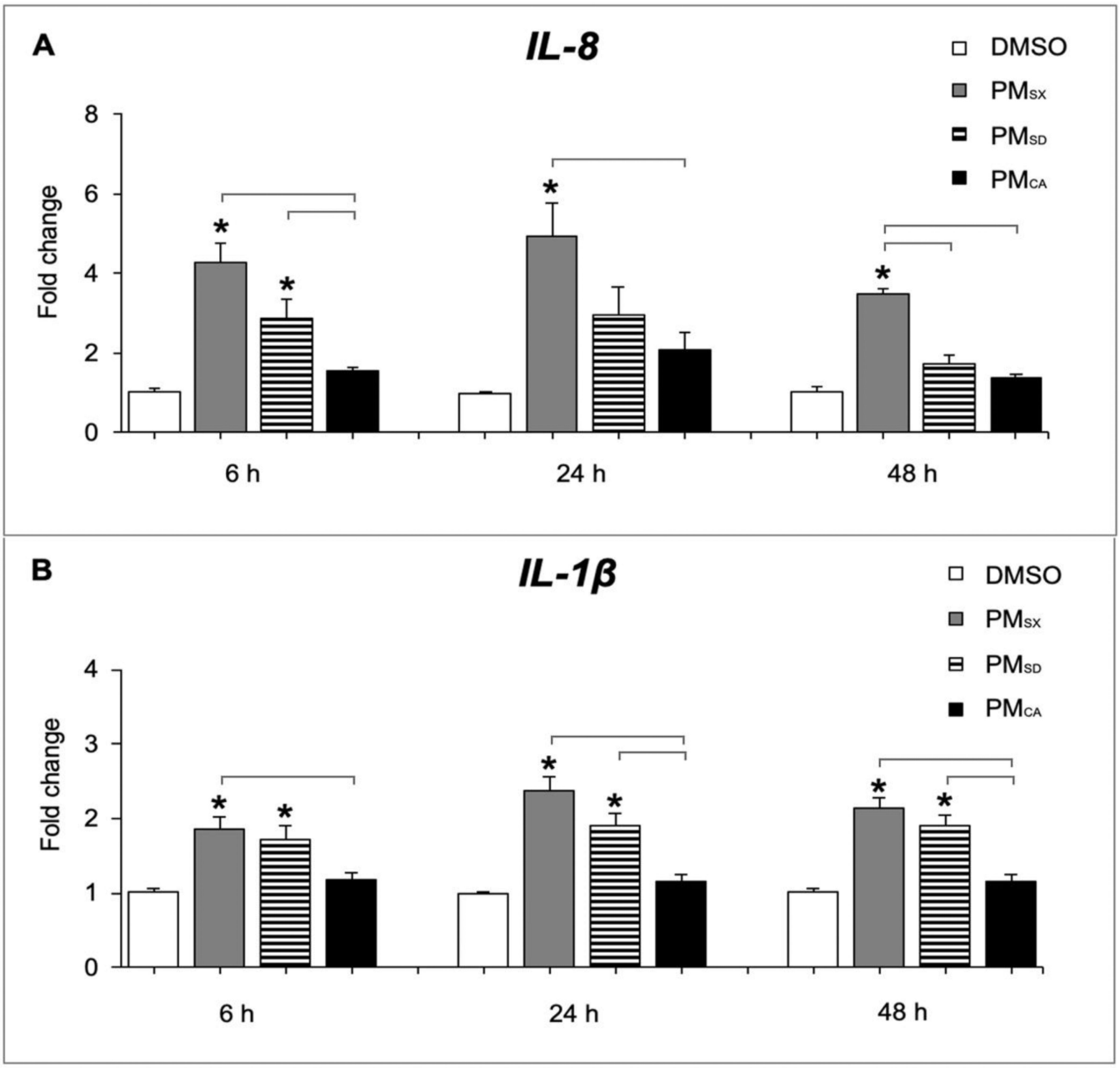


**Figure 7. $PM_{SX}$ significantly increased *IL-8* and *IL-1β* mRNA levels in U937 macrophages following 6, 24, or 48 hours of exposure.**

Graphs show results from qPCR analysis of cells treated with DMSO (control) or PM extracts from Taiyuan, Shanxi ($PM_{SX}$); Jinan, Shandong ($PM_{SD}$); or Sacramento, CA ($PM_{CA}$) for 6, 24, or 48 hours. Gene expression is shown as a fold-change from expression of the housekeeping gene, *ACTB* (beta-actin). Data are shown as mean ± SEM from experiments performed in triplicate. * indicates a significant difference ($p < 0.05$) from control. Brackets indicate significant ($p < 0.05$) differences between non-control groups.

**Table 1:**

ICP-MS Metal concentrations in the Taiyuan, Shanxi ($PM_{SX}$); Jinan, Shandong ($PM_{SD}$); and Sacramento, California ($PM_{CA}$) extract samples.

| | Elemental Concentration (ppm) in Each Extract Sample | | |
|---|---|---|---|
| **Element** | **$PM_{SX}$** | **$PM_{SD}$** | **$PM_{CA}$** |
| Potassium (K) | 12 | 12 | 15 |
| Calcium (Ca) | 19 | 5.2 | 7.6 |
| Zinc (Zn) | 3.6 | 2.1 | 3.7 |
| Copper (Cu) | 0.054 | 0.12 | 2.1 |
| Magnesium (Mg) | 14 | 1.1 | 1.7 |
| Iron (Fe) | 0.66 | 0.34 | 1.1 |
| Lead (Pb) | 0.36 | 0.31 | 0.046 |
| Nickel (Ni) | 0.015 | 0.023 | 0.027 |

PM samples were collected during the winter season and extracted prior to analysis.

**Table 2.**

HR-AMS bulk composition of Taiyuan, Shanxi ($PM_{SX}$); Jinan, Shandong ($PM_{SD}$); and Sacramento, California ($PM_{CA}$) extract samples*.

| Chemical Group | $PM_{SX}$ | $PM_{SD}$ | $PM_{CA}$ |
|---|---|---|---|
| Organics | 44 | 57 | 54 |
| Nitrate | 11 | 15 | 32 |
| Sulfate | 26 | 14 | 2.0 |
| Ammonium | 13 | 9.0 | 11 |
| Chloride | 6.0 | 5.0 | 1.0 |

*Numbers represent percentages of the total PM mass. PM samples were collected during the winter season and extracted prior to analysis.

**Table 3.**

Elemental Composition of Organics.

| Element | $PM_{SX}$ | $PM_{SD}$ | $PM_{CA}$ |
|---|---|---|---|
| C | 59 | 62 | 46 |
| O | 31 | 26 | 45 |
| H | 8.5 | 11 | 7.0 |
| N | 1.7 | 1.6 | 1.5 |

Carbon (C), oxygen (O), hydrogen (H), and nitrogen (N) content in wintertime PM extracts from Taiyuan, Shanxi ($PM_{SX}$); Jinan, Shandong ($PM_{SD}$); and Sacramento, California ($PM_{CA}$). Characterization was performed using high-resolution time-of-flight aerosol mass spectrometry. Numbers above are percentages of the total organic mass.